EasyChair Preprint

№ 7754

Thermal Characteristics and Icing Risk Analysis of Tethered Airships at Medium and Low Altitudes

Lin Junyaun, Xu Zhehan, Liu Qiang, Fang Xiande and Dai Qiumin

April 10, 2022

Thermal characteristics and icing risk analysis of tethered airships at medium and low altitudes

Lin Junyuan[1], Xu Zhehan[1], Liu Qiang[2], Fang Xiande[3], Dai Qiumin[1],*

[1]School of Energy and Power Engineering, Nanjing University of Science and Technology, Nanjing 210094, China

[2]Aerospace Information Research Institute, Chinese Academy of Sciences, Beijing 100094, China

[3]School of Aerospace Engineering, Nanjing University of Aeronautics and Astronautics, Nanjing 210019, China

Abstract. In order to analyze the risk of icing that is affected by supercooled water droplets when the tethered airship hovering at mid-low altitude, the airship envelope was simplified as a boundary without wall thickness. The solar and infrared radiant heat transfer was loaded by Fluent-UDF, while the convective heat transfer inside and outside the envelope was obtained by coupled boundary method. The thermal characteristics of the tethered airship was numerical simulated. Based on which, the electric heating anti-icing analysis was conducted. The results show that, the temperature of the envelope is lower than the freezing point on the vernal equinox and winter solstice at 4km with wind speed of 10 m/s. While on summer solstice, the icing risk of the envelope is relative low. The envelope temperature may be increased effectively by adopting heating at the key area of the envelope.. The research conclusions provide a certain basis for improving the safety of the airship.

Keywords. Airship, Simulation, Thermal Characteristics, Icing risk

1 Introduction

With the inherent capability of hovering at medium and low altitudes for months， the tethered airships have wide application prospects in the fields of environmental protection, border monitoring and early warning communication [1-2]. Since the working altitude is generally below 6km, where the atmosphere is full of supercooled water droplets and clouds, the tethered airship may encounter high risk of icing on the envelope. The aerodynamic characteristics of the airship may be deteriorated and the weight balance may be destroyed when the envelope of the airship freezes, leading serious threat to the safety of the tethered airships.

Affected by the environmental factors, the temperature distribution of the envelope is uneven and may be easily disturbed. Therefore, the icing characteristics of the airship is different from that of the

* Corresponding author.
E-mail: daiqiumin@njust.edu.cn.

traditional aircraft. At present, there are few studies on the icing characteristics of aerostat. In July 2011, the high-altitude long-endurance aerostat demonstration boat (HALE-D) ascent test was failed when the aerostat reaches the altitude of 9.9km[3]. It was confirmed that the failure was caused by the exhaust accident when the exhaust valve was blocked by ice. Liu et al. [4] calculated the icing behavior of the airship when it crossed the cumulonimbus cloud after launching, and the results showed that when the airshipreaches altitude of 3 km, there was a possibility of icingon the windward side of the airship and the leading edge of the tail. the larger of water collection coefficient, the thicker of the ice. The icing quality is linearly proportional to the time. Thermal characteristics of the airship show unlegctable effcct on the icing behaviors. Therefore, the study of the thermal characteristics of the airship is the basis of icing analysis.

At present, the research on thermal characteristics of airships lacks of coupling analysis with other physical fields. Therefore, the coupled analysis of the internal and external flow fields and thermal characteristics of the airship is carried out to obtain the distribution law of the flow field and temperature field. The possibility of icing on the surface of the airship can be judged to determine its risk.

For the coupling analysis of the later thermal characteristics and icing characteristics, structural deformation, thermal motion and other multi-physics fields, this paper conducts a coupled analysis of the thermal characteristics of the aerostat and the internal and external flow fields based on Fluent. The loading of solar radiation and long-wave radiation on the skin surface and the coupling calculation of internal and external convection heat transfer are realized through User Defined Function (UDF) and no-thickness boundary setting. This question will be used to explore effective anti-icing solutions.

2 Theory and Computational Methods

The thermal factors that affecting the tethered airship is shown in Fig. 1.

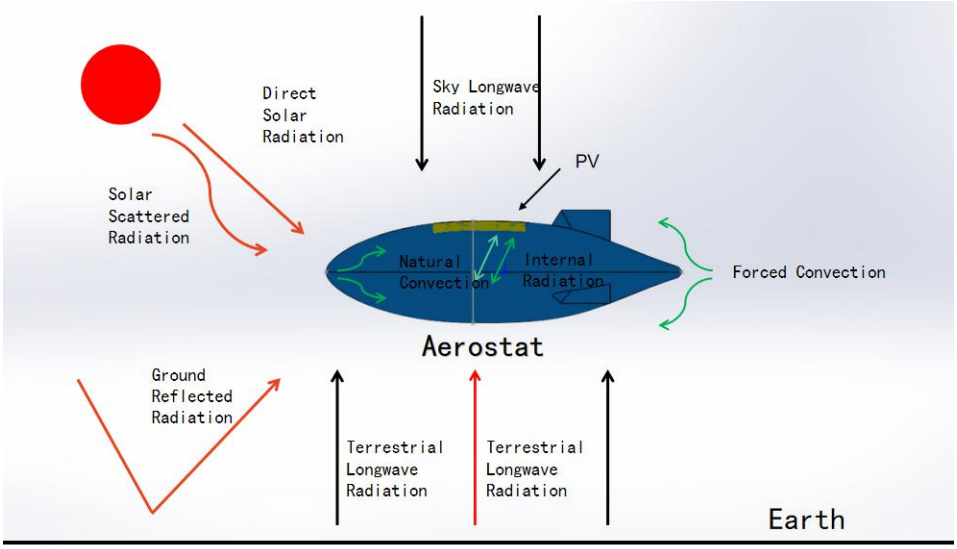

Fig.1 Thermal environmental factors of aerostat

The thermal environment factors of the aerostat mainly include solar radiation, infrared radiation and convection heat transfer. Since the ideal convective heat transfer equations are normally fitted by averaged Nu of the Simple geometry with constant temperature or heat flux, the convective heat transfer obtained by the ideal equations may lead to remarkable errors. Therefore, in order to obtain the accurate temperature distribution of the skin surface, the coupling calculation of the internal and external flow fields and the skin is necessary.

It can be seen from the above figure that the thermal environment factors of the aerostat mainly include solar radiation, long-wave radiation and convection heat transfer. For an ideal atmosphere, the calculation error of the convective heat transfer of the airship is the largest. Because the calculation of convective heat transfer on the skin surface is based on the constant temperature or constant heat flow average convective heat transfer calculation formula of simple geometry, on the one hand, simple geometry cannot accurately describe the shape characteristics of the airship; on the other hand, based on the average convective heat transfer coefficient The calculation is also not conducive to the analysis of the temperature distribution of the skin surface. Therefore, in order to obtain the accurate temperature distribution of the skin surface, the coupling calculation of the internal and external flow fields and the skin is necessary.

2.1 Flow field modeling and skinning

The length of tethered airship adopted in this paper is 151, while its maximum radius is about 21

m. The computational domain, which is divided into helium zone and air zone, is shown in Fig.2. The tethered airship is located in the center of the cylinder. The velocity inlet is 225 meters from the head of the airship, the outflow is 675 meters from the tail of the airship. The radius of the computational domain is 100 meters.

The external and internal convictive heat transfer can be obtained by adopting coupling boundary. In order to solve the conflict between the large-scale flow field and the small-scale skin thickness, the skin can be simplified as a non-thickness wall. At the same time, based on the consideration of the envelope thickness, the temperature gradient in the thickness direction of the envelope can be ignored. The solar radiation and infrared radiation profile can be loaded by the Heat Generation Rate User-Defined-Function(UDF).

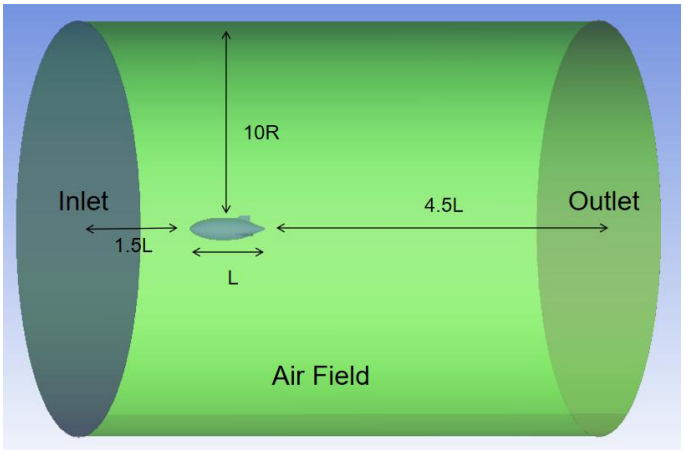

Fig. 2 Computational domain inside and outside the aerostat

2.2 Analysis of key areas of icing and simulation of heat flow

When the tethered airships encounter supercooled water droplets and clouds, the icing process on the envelope can be divided into three steps: (1) The supercooled water droplets flow in the flow field around the aerostat and impinge on the windward side of the aerostat. (2) Some of the supercooled water droplets that hit the windward side of the aerostat adhere to the envelope and generate water film flow. Other water droplets are bounced and splashed off the surface of the aerostat; (3) The water film attached on the envelope turn into ice because of heat transfer Therefore, the size of the water droplet coefficient on the envelope indicates the amount of ice on the airship. Affected by the air flow, the windward side of the airship, such as head of the airship and the leading edge of the tail, were considered to be as key area with high risk of icing.

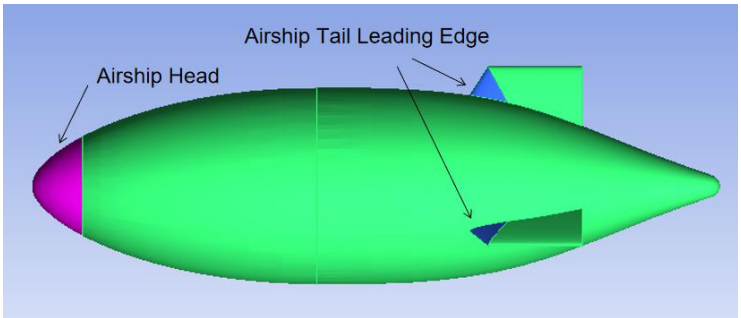

Fig. 3 Division of key areas of icing

UDF [5] in Fluent can be used to customize boundary conditions, define material properties, define surface and volume reaction rates. It also can be used to load solar radiation, infrared radiation and extra heat flux profile on the envelope. Extra heat flux profile loaded on the envelope can be used to verify the anti-ice Feasibility.

2.3 Governing equation and calculation method

Because the wind speed is relatively low, steady-state incompressible Navier-Stokes equations can be used to describe the internal and external flow fields of the aerostat. The general control equation is expressed as:

$$\text{div}\,(\rho \boldsymbol{u}\phi) = \text{div}\,(\Gamma \text{grad}\,\phi) + S \tag{1}$$

where ρ is the gas density, u is the velocity vector; ϕ is a universal variable, Γ is the generalized diffusion coefficient, S is the source term, and its specific expression is shown in Table 1.

Table 1 Specific expressions of control equations

Equation	Universal variable Φ	Diffusion coefficient Γ	Source S
Continuity equation	$\phi = 1$	$\Gamma = 0$	$S = 0$
Momentum equation in the x direction	$\phi = u_x$	$\Gamma = \mu_{eff} = \mu + \mu_t$	$S = -\partial p/\partial x + 1/3\partial(\mu_{eff}\text{div}u_x)/\partial x$
y-direction momentum equation	$\phi = u_y$	$\Gamma = \mu_{eff} = \mu + \mu_t$	$S = -\partial p/\partial y + 1/3\partial(\mu_{eff}\text{div}u_y)/\partial y$
z-direction momentum equation	$\phi = u_z$	$\Gamma = \mu_{eff} = \mu + \mu_t$	$S = -\partial p/\partial z + 1/3\partial(\mu_{eff}\text{div}u_z)/\partial z - \rho g$
energy equation	$\phi = T$	$\Gamma = \mu / Pr + \mu_t / \sigma_T$	$S = 0$

wehre μ_{eff} is the total turbulent viscosity, μ_t is the turbulent viscosity, μ is the gas viscosity

coefficient, p is the pressure.

The energy source term S_{T_En} can be calculated as:

$$S_{T\_En} = (q_{En\_D} + q_{En\_Atm} + q_{En\_Ear} + q_{En\_IR\_Ex})/d \quad (2)$$

where q_{En_D} is the absorbed direct solar radiation heat flow, q_{En_Atm} is the absorbed atmospheric scattered solar radiation heat flow, q_{En_Ear} is the absorbed surface reflected solar radiation heat flow, $q_{En\_IR\_Ex}$ is the long-wave radiation heat exchange heat flow with the atmosphere or the earth, and d is the envelope thickness .

The RNG k-ε turbulence model was selected in the simulation calculation, the air and helium density models are incompressible ideal gases, the Velocity Inlet is selected as the inlet, the Pressure Outlet is set as the outlet, the boundary is the boundary of the Symmetry Plane, the pressure coupling method is selected as the SIMPLE solution, and the rest use the Second-order Upwind scheme.

2.4 Grid Independence Verification

Before the calculation, the independence of the grid should be verified.The appropriate number of grids should be selected to reduce the occupation of computer memory resources and reduce the calculation time. In this paper, ICEM is used to perform unstructured meshing of the computational domain, and boundary layer meshes are set in the area near the wall. Taking the calculation time at 0:00 on the vernal equinox as an example, the total number of grids is 1.16 million, 1.97 million, 2.75 million and 3.55 million. Compared with the calculation results of 4.33 million hours, the relative errors of the near-wall velocity and the average temperature of helium are1.15% and 0.022%,. The calculation results are shown in Table 2. It can be seen that the number of grids of the model meets the calculation requirements when the number of grids is 3.55 million. At this time, the grid section of the inner and outer flow fields is shown in Fig. 4.

Table 2 Calculation results and error comparison of different grids

Number of grids (millions)	$v(m/s)$	Relative error(%)	$T(K)$	Relative error(%)
0.86	0.410	5.31	265.83	0.162
1.97	0.415	4.15	265.23	0.064
2.75	0.446	3.00	265.54	0.052
3.55	0.438	1.15	265.46	0.022
4.33	0.433	-	265.40	-

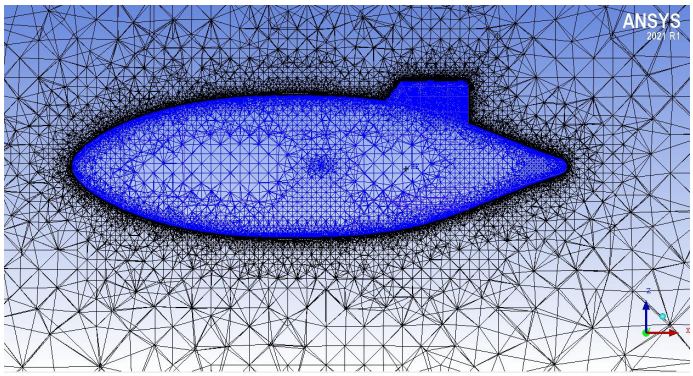

Fig. 4 Grid section of internal and external flow fields

3 Simulation results

Three typical dates were chosen for analysis. namely the spring equinox, the summer solstice, and the winter solstice, and the location was 4 km above Nanjing. The simulation model selects a Y-shaped tail aerostat, the skin area is 16722 m^2, the envelope solar radiation absorptivity is 0.18, the skin infrared radiation absorptivity is 0.8, the skin thickness is 0.1 mm, the atmospheric wind speed is 10m/s.

3.1 Analysis of thermal characteristics of airship

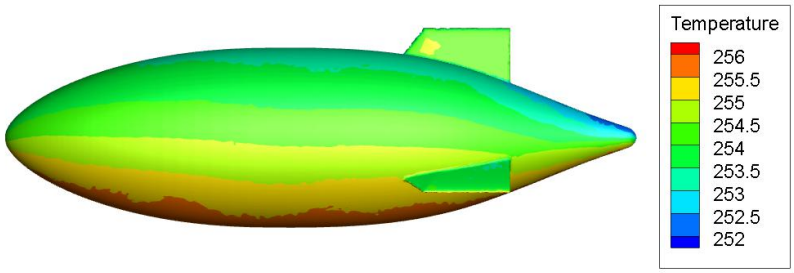

Fig.5 envelope temperature distribution on winter solstice

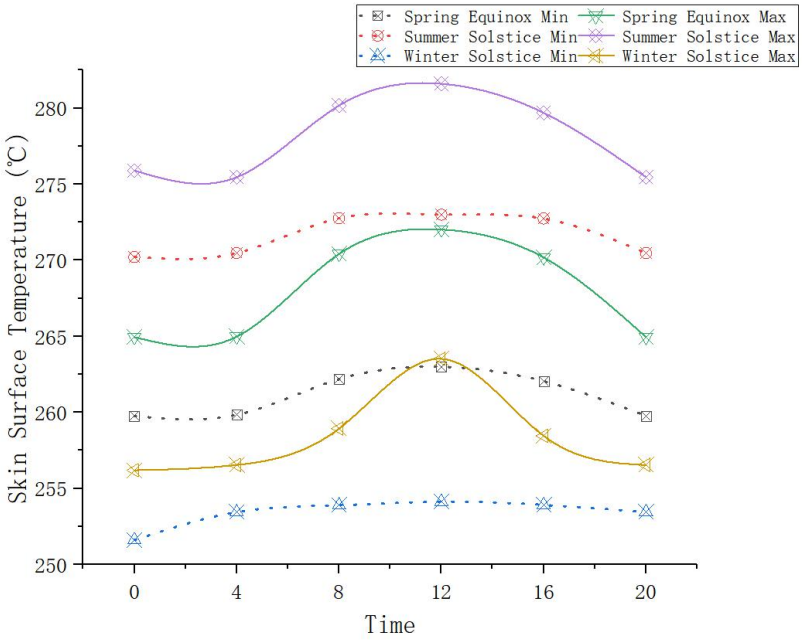

Fig.6 Temperature variaiton of envelope

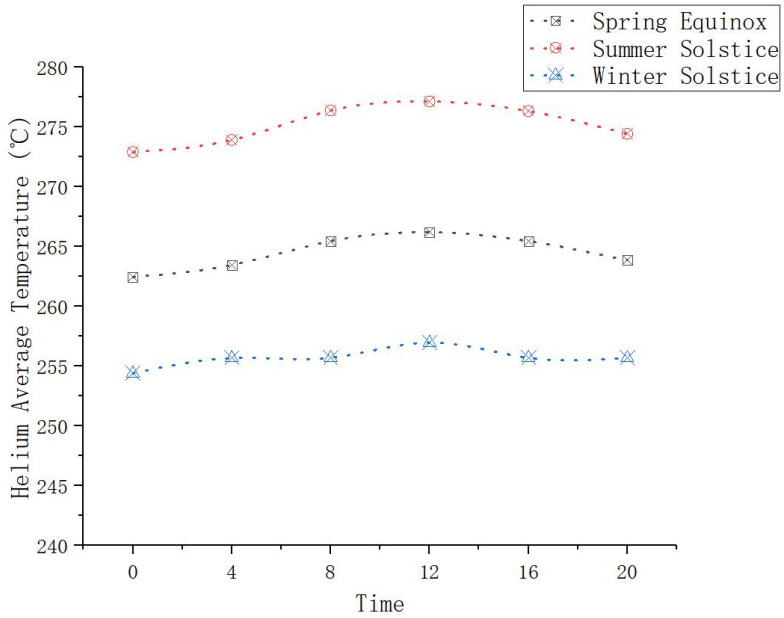

Fig.7 Helium average temperature variation

When the airship is in the air, the surface temperature of the envelope and the temperature of the helium gas vary with time, and the temperature difference between day and night is large. When the skin temperature is lower than 273.15K, there is the possibility of freezing. The temperature of the skin surface and the helium temperature at different time points in three typical seasons are shown in Fig.5 to Fig.7.

At 0:00 on the winter solstice , from Fig.5 ,it can be seen the temperature of the skin decreases from the bottom to the top of the airship. The minimum temperature of the skin is 251.2K, and the

temperature difference of the skin is 3-5K.The reason is the long-wave radiation on the ground is the only heat source of the aerostat at night, the bottom of the skin is higher than that at the top. At this time, the overall temperature of the aerostat is less than 275.15K, and there is the possibility of freezing. The location, scope and size of the freezing will be different with the air speed and the water content.

From Fig.6 and Fig.7, the temperature of the skin surface changes at each time point on the vernal equinox, summer solstice and winter solstice can be known. The temperature change trend is roughly the same, showing periodic changes. On the vernal equinox and winter solstice, the minimum temperature of the skin is 259.76K and 251.6K, respectively, and the maximum temperature of the skin is 272.02K and 263.52K. In the same season, the maximum temperature difference is about 8K. Compared with the temperature change in the stratosphere, the reason is, in the troposphere, the influence of radiation is more balanced, and the temperature difference caused by it is also small. Because of he skin temperature is all lower than 273.15K, and the helium temperature is also below 273.15K, the whole airship has the possibility of freezing. On the summer solstice, the maximum and minimum temperatures of the skin are 281.6K and 270.2K , the maximum and minimum temperatures of the helium temperature are 272.92K and 277.15K, the average temperature is greater than 273.15K, and the airship may be icing or non-icing condition.

3.2 Analysis of Electric Heating Simulation Results

There is a greater risk of icing during the mid-low-altitude tethered airship's airborne operation. Combined with the distribution of the water droplet collection coefficient in Reference 9, an additional heat flow of 100 W/m^2 was applied to the windward side of the airship's head and tail ,through the result to analyze the influence of electric heating on thermal characteristics and icing risk.

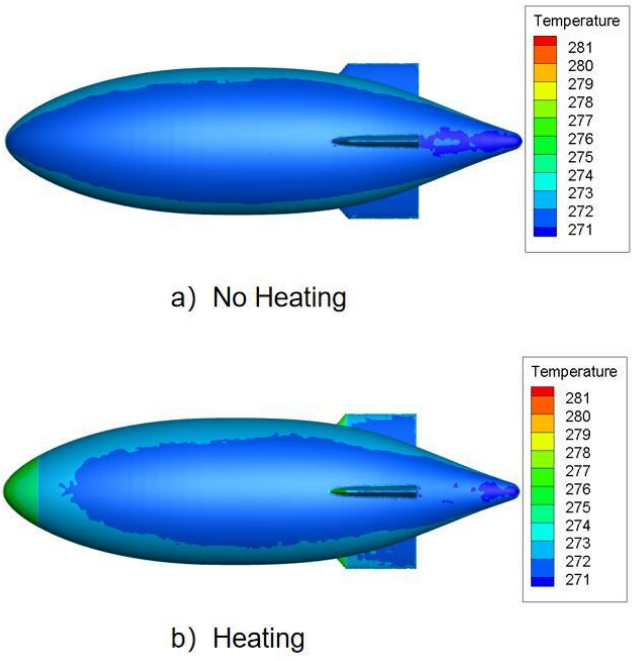

Figure 8. Cloud diagram of temperature distribution of skin with or without electric heating a) No heating b) With heating

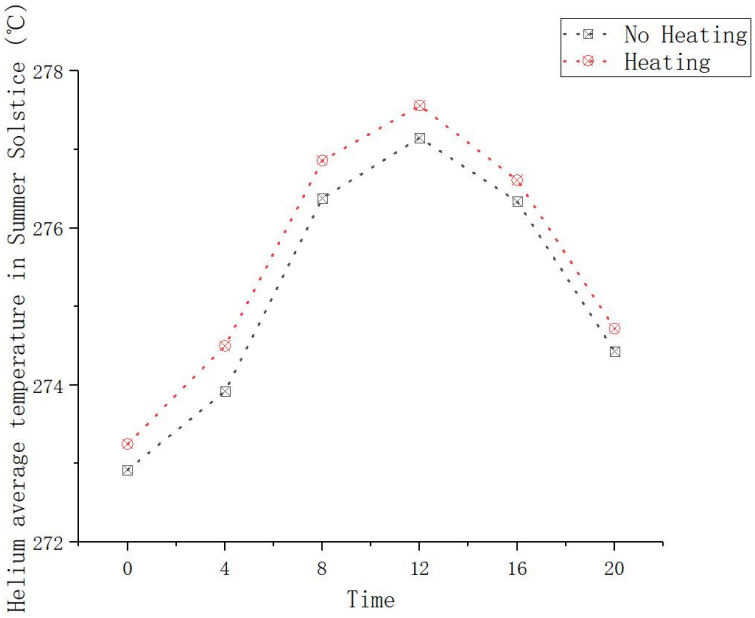

Figure 9 Helium temperature comparison

In the thermal analysis in the previous section, it can be known most of the airships have the possibility of freezing, and only during the summer solstice may there be no ice, so the summer solstice is selected as the time point for the electric heating simulation. The additional heat flow applied to the key icing area is to increase the temperature of the icing area above the freezing point ,the aim is to reduce the amount of icing in freezing area. The temperature distribution with and without heating is

shown in Fig. 8.

From Fig.8,the temperature distribution of the airship with and without heat flow is applied. The comparison of the distribution shows the skin outside the heating area has little effect on the heat,the skin temperature gradually increases from the upper end to the lower end of the airship. Before applying the heat flow, the temperature of the icing key area was about 271K. After applying the heat flow, the temperature difference of the skin surface increased by 5K, and the temperature of the key area was greater than 273.15K. From Fig. 9,the temperature of the helium gas after applying the heat flow increases by about 0.3K on average. Therefore, on the summer solstice, electric heating can effectively change the surface temperature of the skin.

4 Conclusion

Based on the Fluent simulation software and User-Defined-Functions (UDFs), the physical model and thermal characteristic model of the aerostat was established. The thermal environment of the airship was accurately described. The simulation on the thermal characteristics of medium-low altitude tethered airships was conducted, and an anti-icing mode combined with electric heating was proposed. The temperature distributions of the envelope， helium temperature variation and icing risk at typical seasons was analyzed. The conclusions are as follow

(1) On the vernal equinox and winter solstice, the airship has a high risk of icing. While on the summer solstice, the icing risk is relatively low..

(2) After applying the heat flux, the temperature of the key area on the envelope increases by 5K, which reduces the icing risk of the envelope.

Based on the simulation software, the thermal characteristics and both of external and internal flow filed can be obtained by coupling analyze. The electric heating anti-icing method can improve the safety of the mid- and low-altitude airship.

Acknowledgement

This paper was supported by National Key Research and Development Program of China (No.2018YFB0504805-5), Key program of National Natural Science Foundation of China (No. 61733017), Youth Innovation Promotion Association of Chinese Academy of Sciences (2020133), Strategic Priority Research Program of China Academy of Sciences (No. XDA17020101), Key program of Aerospace Information Research Institute, Chinese Academy of Sciences (No. Y9K0230Z2F).

references:

[1] Peng Guilin, Wan Zhiqiang. Status and prospect of remote sensing and telemetry applications of aerostats in China [J]. Journal of Earth Information Science, 2019, 21(04): 504-511.

[2] Zhang Yongjun. Geometric processing of low-altitude remote sensing images of unmanned airships [J]. Journal of Wuhan University (Information Science Edition), 2009, 34(03): 284-288.

[3] Androulakakis S P. Status and plans of High Altitude Airship (HAATM) Program[R]. AIAA 2013-1362, 2013.

[4] Qiang Liu, Yanchu Yang, Qian Wang, et al. Icing performance of stratospheric airship in ascending process[J]. Advances in Space Research,2019,64(11):2405-2416.

[5] http://www.ansys.com/Resource+Library.